



Evaluation of critical parameters in the hollow-fibre system for tuberculosis: A case study of moxifloxacin

Diana A. Aguilar-Ayala¹ | Fernando Sanz-García¹  |
Marie Sylvianne Rabodoarivelo¹ | Budi O. Susanto² | Rebeca Bailo¹ |
Maxime R. Eveque-Mourroux³ | Nicolas Willand³ | Ulrika S. H. Simonsson² |
Santiago Ramón-García^{1,4,5}  | Ainhoa Lucía^{1,4} | on behalf of the ERA4TB consortium

¹Department of Microbiology, Pediatrics, Radiology and Public Health, University of Zaragoza, Zaragoza, Spain

²Department of Pharmaceutical Biosciences, Uppsala University, Uppsala, Sweden

³Univ. Lille, Inserm, Institut Pasteur de Lille, U1177 - Drugs and Molecules for Living Systems, Lille, France

⁴Spanish Network for Research on Respiratory Diseases (CIBERES), Carlos III Health Institute, Madrid, Spain

⁵Research and Development Agency of Aragón (ARAID) Foundation, Zaragoza, Spain

Correspondence

Santiago Ramón-García, Research and Development Agency of Aragón (ARAID) Foundation, Zaragoza, Spain.

Email: santiramon@unizar.es

Ainhoa Lucía, Department of Microbiology, Pediatrics, Radiology and Public Health, University of Zaragoza, Zaragoza 50009, Spain.

Email: ainhoalq@unizar.es

Funding information

European Union, Innovative Medicines Initiative 2 Joint Undertaking, Grant/Award Number: No 853989; Gobierno de Aragón Spain, Grant/Award Number: Ref.LMP132_18

Aims: The hollow-fibre system for tuberculosis (HFS-TB) is a preclinical model qualified by the European Medicines Agency to underpin the anti-TB drug development process. It can mimic in vivo pharmacokinetic (PK)-pharmacodynamic (PD) attributes of selected antimicrobials, which could feed into in silico models to inform the design of clinical trials. However, historical data and published protocols are insufficient and omit key information to allow experiments to be reproducible. Therefore, in this work, we aim to optimize and standardize various HFS-TB operational procedures.

Methods: First, we characterized bacterial growth dynamics with different types of hollow-fibre cartridges, *Mycobacterium tuberculosis* strains and media. Second, we mimicked a moxifloxacin PK profile within hollow-fibre cartridges, in order to check drug-fibres compatibility. Lastly, we mimicked the moxifloxacin total plasma PK profile in human after once daily oral dose of 400 mg to assess PK-PD after different sampling methods, strains, cartridge size and bacterial adaptation periods before drug infusion into the system.

Results: We found that final bacterial load inside the HFS-TB was contingent on the studied variables. Besides, we demonstrated that drug-fibres compatibility tests are critical preliminary HFS-TB assays, which need to be properly reported. Lastly, we uncovered that the sampling method and bacterial adaptation period before drug infusion significantly impact actual experimental conclusions.

Conclusion: Our data contribute to the necessary standardization of HFS-TB experiments, draw attention to multiple aspects of this preclinical model that should be considered when reporting novel results and warn about critical parameters in the HFS-TB currently overlooked.

Diana A. Aguilar-Ayala and Fernando Sanz-García were equal first author contributors. Santiago Ramón-García and Ainhoa Lucía were equal last author contributors.

This is an open access article under the terms of the [Creative Commons Attribution-NonCommercial-NoDerivs](https://creativecommons.org/licenses/by-nc-nd/4.0/) License, which permits use and distribution in any medium, provided the original work is properly cited, the use is non-commercial and no modifications or adaptations are made.

© 2024 The Authors. *British Journal of Clinical Pharmacology* published by John Wiley & Sons Ltd on behalf of British Pharmacological Society.

1 | INTRODUCTION

The hollow-fibre system for tuberculosis (HFS-TB) is currently the only preclinical tool qualified by the European Medicines Agency and it is endorsed by the Food and Drug Administration for tuberculosis (TB) drug development.^{1–3} This *in vitro* assay allows to study a continuous culture of *Mycobacterium tuberculosis* that grows in an enclosed bioreactor (i.e. a hollow fibre cartridge), which is exposed to drugs where their pharmacokinetic (PK) profile (i.e. the concentration vs. time profile in human plasma or the site of infection) can be mimicked *in vitro* within the cartridge.^{4,5} This cartridge is comprised of an extracapillary space (ECS) where bacteria are housed, also referred to as the pharmacodynamics (PD) compartment, and an intracapillary space (ICS), also dubbed the PK or central compartment. Most compounds, nutrients and bacterial metabolites freely traverse and equilibrate with the ECS via diffusion across the semipermeable fibres' pores, if the molecular weight cut-off of said fibres allows it.^{6,7} This molecular weight cut-off enables the replenishment of media at a fixed rate and the addition or clearance of drugs to and from the ECS, while *M. tuberculosis* cells stay confined. By mimicking the human PK of an antibiotic in the system, preclinical HFS-TB readouts might predict clinical therapeutic events using PKPD modelling.⁸ Furthermore, the HFS-TB does not raise the ethical concerns that animal models do and it allows reaching bacterial density in accordance with *in vivo* infections. It also allows iterative and repetitive sampling to produce longitudinal data, which have been shown to be more informative than single time point estimates of efficacy; thus, improving statistical power to identify PKPD relationships.⁹ Further, it has the advantage of not being time-limited, which enables the quantification of the emergence of resistance for a particular drug.^{10–12}

The importance of HFS-TB also rests with its potential role to contribute to the PKPD characterization of new drugs and regimens to improve the current therapy against TB. Longitudinal PKPD data at site of action for novel agents against *M. tuberculosis* are difficult to obtain in a clinical context due to the invasive nature of the procedure, that is, lung resection.^{13,14} In this context, HFS-TB stands as a very useful tool to boost the TB drug development process. For example, it can inform the PKPD driver for antimicrobial activity of the unbound drug fraction, that is, maximal concentration (C_{max}), area under the concentration–time curve (AUC) or percentage of time (T) over the minimal inhibitory concentration (MIC), that is, C_{max}/MIC , AUC/MIC or %fT/MIC, respectively. In addition, different dosing schedules can be mimicked (i.e. once daily, QD vs. twice daily, BID) to inform clinical designs.^{15–17} HFS-TB research has centred so far on novel anti-TB compounds,¹⁸ combinations in preclinical stages¹⁹ or repurposed molecules,^{20,21} among other approaches. Concerning the latter, newer fluoroquinolones have a promising future as first-line agents against TB, including multidrug-resistant TB.^{22,23} Among them, moxifloxacin's encouraging antimycobacterial activity has led to recent clinical trials, where this drug was given alone or in combination with other drugs, in order to evaluate its efficacy.^{24,25} Hence, the imperative need to optimize moxifloxacin dosing strategies has given rise to a number of HFS-TB studies.^{12,18,19,26,27}

What is already known about this subject

- The hollow-fibre system for tuberculosis (HFS-TB) is a useful preclinical model that can inform the design of clinical trials.
- Historical data and published protocols are insufficient for interlaboratory reproducibility, and many parameters that can affect conclusions are normally omitted.

What this study adds

- Our study evaluates, for the first time, critical parameters in the HFS-TB that have traditionally been overlooked and may impact experimental conclusions.
- Drug–fibres compatibility tests need to be run before actual HFS-TB assays.
- The sampling method and the bacterial adaptation period before drug infusion impact conclusions.

Despite the advantages and potential benefits that HFS-TB could offer to public health strategies, this methodology is still quite novel. It was first presented in 2004¹⁰ and has only been exploited by a few research groups. In this sense, although there exist methodological guidelines, no comprehensive recommendations, standard procedures or mandatory quality control steps are established in the field. In fact, most studies provide insufficient data for interlaboratory reproducibility, with key parameters needed for data interpretation not reported.^{1,5,28} For instance, the chemical properties of the molecule(s) under study may cause nonspecific bindings to the fibres or other elements of the system. In addition, there are several factors that can possibly impact PKPD such as growth media, type of cartridge, bacterial strain, inoculum size, sampling method or bacterial adaptation time before drug infusion. All taken together, there are numerous factors that have not been properly discerned nor systematized in this methodology.^{10,28}

With the aim of standardizing HFS-TB operational procedures, the goal of this study was to characterize the impact of strains, the cartridge's composition and size and bacterial adaptation times on the moxifloxacin killing rate in HFS-TB.

2 | METHODS

2.1 | Bacterial strains, growth conditions and drugs

Previously quantified stocks—as indicated in previous works²⁹—of *M. tuberculosis* H37Ra (ATCC25177; American Type Culture Collection), with an optical density at 600 nm (OD_{600}) of 0.6, which

correspond to $\sim 5.1 \times 10^6$ colony-forming units (CFU)/mL; and *M. tuberculosis* H37Rv (Pasteur Institute strain, NCBI Genome reference NC_000962.3), with $OD_{600} = 0.6$, $\sim 1.1 \times 10^7$ CFU/mL, stored at -80°C , were used in our assays. Unless otherwise stated, bacteria were grown in Middlebrook 7H9 broth (Becton Dickinson, New Jersey, USA) supplemented with 10% (vol/vol) Middlebrook oleic acid-albumin-dextrose-catalase (OADC; Becton Dickinson, New Jersey, USA), 0.5% (vol/vol) glycerol (Scharlau, Hamburg, Germany) and 0.05% (vol/vol) tyloxapol (Sigma-Aldrich, St. Louis, USA), from now on abbreviated as 7H9/OADC/Gly/Tx, or in plates containing Middlebrook 7H10 agar (Becton Dickinson, New Jersey, USA) supplemented with 10% (vol/vol) OADC (Becton Dickinson, New Jersey, USA), 0.5% (vol/vol) glycerol (Scharlau, Hamburg, Germany) and 0.05% (vol/vol) tyloxapol (Sigma-Aldrich, St. Louis, USA), from now on abbreviated as 7H10/OADC/Gly/Tx, at 37°C without CO_2 .

Moxifloxacin and rifampicin (European Pharmacopoeia Reference Standard, Y0000703 and R0700000, respectively) stock solutions were dissolved in sterile water and dimethyl sulfoxide, respectively, on the day of the experiment. Subsequently, drug aliquots were diluted to the required concentration in 7H9/OADC/Gly/Tx and used immediately. Note that both drugs maintain their stability after 3 freeze–thaw cycles.^{30,31} Further, all bioanalyses in this work included a drug stock control and the syringe's solution, which contains the drug in the broth media. These controls have barely differed from their expected concentrations, prepared before the freeze–thaw cycle, which validates the stability of the compounds in these conditions.

2.2 | HFS-TB materials and set up

A schematic representation of the HFS-TB can be found in Sadouki *et al.*⁵ Further, all materials, their technical specifications and their role in the HFS-TB assembly are encompassed in Table S1. All the bottles, caps, media, tubing, fittings and filters indicated in Table S1 were autoclaved before each experiment. A sterility test was performed on the culture media, by placing it both at room temperature and 37°C for 1 week. According to manufacturer's recommendations (FiberCell Systems, New Market, USA), Duet pumps were set at a rate of 25 U (~ 100 – 110 mL/min) for medium-size cartridges and 10 U (~ 50 mL/min) for the small-size cartridges to allow rapid distribution and equilibration of broth and drug between the ECS and the ICS. All HFS-TB experiments underwent a preconditioning step of 3–4 days without broth dilution before bacteria inoculation and/or antibiotic infusion, in order to properly hydrate the fibres by means of the Duet pump's recirculation. On the day of system's assembling, the peristaltic pump was turned on at a high rate to ensure there were no leakages throughout the circuit. System volume was 200 mL. Mixing of the ECS content through S2 and S3 ports was carried out before each PKPD sampling and every other day, using 3-body Luer-Lock syringes of 20 or 3 mL (BBraun, Melsungen, Germany) for medium-size or small-size cartridges, respectively. The 20-mL syringes were also utilized for drug administration. An overview of drug concentrations in

the syringes and injection regimens is shown in Table S2. For sampling, 3-body Luer-Lock 1-mL syringes (ThermoFisher Scientific, Waltham, USA) were used. PK samples were stored at -20°C until quantitation.

2.3 | Bacterial growth in the HFS-TB

Unless otherwise stated, 10^5 CFU/mL from a quantified stock of *M. tuberculosis* H37Ra or *M. tuberculosis* H37Rv were incubated in 7H9/OADC/Gly/Tx in a sterile polystyrene flask (TPP, Trasadingen, Switzerland) at 37°C without CO_2 for 3–4 days, in order to achieve exponential phase ($\sim 10^6$ CFU/mL). Concurrently, the HFS-TB was assembled and preconditioned for 3–4 days, as previously described. After this step, the bacterial suspension was distributed as follows: 10 mL were placed in a flask for growth control, and a volume matching the cartridge's capacity was introduced with a syringe through the S2 port. Manual homogenization of the ECS content was carried out right after inoculation, and every other day. Twenty-four hours after inoculation, broth dilution was set at a rate of 0.18 mL/min, replacing the diluent and waste reservoirs when needed. Bacterial sampling from the flask and the cartridge was done on the days indicated in Table S3. When indicated, 200 μL of culture were withdrawn from the flask, S2 and S3 ports, 10-fold diluted and placed for subsequent colony counting, as reported earlier.²⁹ Plates were incubated at 37°C without CO_2 for 21 days in order to calculate CFU/mL.

2.4 | Mimicking a PK profile in the HFS-TB

Peristaltic and syringe pumps rates were calculated using standard PK equations. The elimination rate constant (k) was derived according to $k = \ln(2)/t_{1/2}$, where $t_{1/2}$ is the half-life of the compound. The clearance (CL) was derived according to $CL = k \times V$, where V is the total volume of the system (200 mL). The drug concentration at time t after infusion (C_t) was derived according to $C_t = C_5 \times e^{-kt}$, where C_5 is the concentration in the infusion syringe divided by the clearance.

A single oral dose of 400 mg of moxifloxacin or 600 mg of rifampicin was mimicked in medium-size PS cartridges (C2011) without bacteria to examine the compatibility of each drug with the fibres. Given that the purpose of this test was only to check the suitability of cartridge vs. drug—with no clinical significance—the HFS pumps were set up to mimic drug total plasma concentrations in human, namely, $C_{\text{max}} = 3.1$ $\mu\text{g}/\text{mL}$, time to C_{max} (t_{max}) = 1.5 h and $t_{1/2} = 13$ h for moxifloxacin^{26,32}; and $C_{\text{max}} = 9$ $\mu\text{g}/\text{mL}$, $t_{\text{max}} = 2$ h and $t_{1/2} = 3.5$ h for rifampicin.^{27,33} In each case, the drug was infused into the system at a rate and concentration that allowed reaching the C_{max} at the corresponding t_{max} . This concentration was kept for 90 min and samples were taken from all ports at 5 time points during this phase, to assess the time when the drug concentration reached the equilibrium between the ECS and the ICS. Subsequently, moxifloxacin dilution

was set at 0.18 mL/min, and 10 more time points were sampled from all ports (Table S4). The rifampicin dilution was set at 0.66 mL/min and 4 more time points were sampled from all ports (Table S4). Drug concentrations within the syringes and software programming of the pumps are shown in Table S2.

2.5 | PKPD assays in the HFS-TB

Three experiments were performed with technical triplicates. First, to study the impact of bacterial adaptation time on PKPD, *M. tuberculosis* H37Ra cells (10^6 CFU/mL from a previously characterize stock) were inoculated in 4 medium-size PS cartridges (C2011) with one biological replicate. The total plasma concentration vs. time PK profile after 400 mg daily oral dosing of moxifloxacin for 10 days was mimicked in 3 cartridges, the fourth being growth control. The first antibiotic infusion was administered at a different moment in each experimental arm: 1, 3 or 7 days after bacterial inoculation in the cartridges. Preinocula growth, PK parameters, peristaltic pumps' routine and HFS-TB handling were as described above. For this experiment, PK sampling (Table S5) was performed from the S1 and S3 ports and only on the cartridges that underwent 1 and 7 days of bacterial adaptation time. PD sampling was performed from the S3 port before the daily drug infusion on the days indicated in Table S3. Bacterial plating was done on 7H10/OADC/Gly/Tx with and without 1.5 µg/mL of moxifloxacin to calculate CFU/mL at each time point and the emergence of resistance (the MIC of *M. tuberculosis* H37Ra and H37Rv to moxifloxacin is 0.5 and 0.25 µg/mL, respectively).

Secondly, to study the impact of cartridges' size on PKPD, *M. tuberculosis* H37Ra cells (10^6 CFU/mL) were exposed for 10 days in a small-size PS (C2025D) cartridge to a dose of moxifloxacin mimicking total concentrations in humans after 400 mg daily oral dosing with 1 biological replicate. Another equivalent cartridge was inoculated with the same number of bacteria but in the absence of moxifloxacin. The bacterial adaptation period to the cartridge before the first moxifloxacin dose was 1 day. Preinocula growth, PK parameters, peristaltic pumps' routine, bacterial plating, sampling ports and HFS-TB handling were the same as indicated in the previous experiment, while the PK and PD sampling schedules are encompassed in Table S5 and Table S3, respectively.

Third, to study the impact of bacterial strain on PKPD, *M. tuberculosis* H37Rv cells (10^6 CFU/mL) were exposed for 10 days in a medium-size PS (C2011) cartridge to moxifloxacin mimicking total concentrations in humans after 400-mg daily oral dosing—1 biological replicate. Another equivalent cartridge was inoculated with the same number of bacteria but in absence of moxifloxacin. The bacterial adaptation period to the cartridge before the first moxifloxacin dose was 1 day. Preinocula growth, PK parameters, peristaltic pumps' routine, bacterial plating, sampling ports and HFS-TB handling were the same as indicated in the previous experiment, while the PK and PD sampling schedules are encompassed in Table S5 and Table S3, respectively.

2.6 | Preparation of drug samples and drug quantification

Samples for drug quantification, obtained from an ECS sheltering bacteria, were decontaminated before quantification by liquid chromatography (LC)–tandem mass spectrometry (MS/MS). First, samples were spun down by centrifugation (18 000 g, 5 min). Then, the pellet was discarded and the supernatant was diluted 15-fold in acetonitrile. Solutions were finally vortexed for 20 s and stored at -80°C until the quantification step. This decontamination procedure was not implemented for drug samples obtained from the ICS or HFS-TB experiments without bacteria. A 7-point calibration curve covering the range of expected moxifloxacin concentrations in the experiment was established under the same conditions (same matrix composition) as the samples to be quantified. Each point of the calibration curve was measured in duplicate covering the range of expected concentrations.

The LC analysis was performed using a ultraperformance LC (UPLC) Acquity I-Class system (Waters, Milford, MA, USA) equipped with an Ethylene Bridge Hybrid C8 analytical column (1.7 µm, 50 mm × 2.1 mm). The elution was performed with a 4-min gradient from 2 to 98% acetonitrile, with a flow rate set at 600 µL/min. The UPLC system was coupled online to a Xevo TQD system (Waters, Milford, MA, USA) equipped with an ESI source. The mass spectrometer was operated in positive ion mode with a specific multiple reaction monitoring (MRM) method for the moxifloxacin compound. The raw data were processed within the MassLynx software version. In addition, bioanalytical LC–MS/MS methods for moxifloxacin and rifampicin were validated for: (i) selectivity and specificity—optimized LC–MS/MS method with specific MRM transitions for each drug; (ii) accuracy and precision—based on the R^2 values obtained for each calibration curves models from all the experiments; all of them $>.999$; (iii) recovery—we barely differ between the expected and the calculated concentrations; and (iv) matrix effect—we used the broth to build the calibration curves to mimic the samples to quantify-ion 4.1 (Waters, Milford, MA, USA).

2.7 | Data analysis

Bacterial burden (\log_{10} CFU/mL) vs. time data (417 observations) was compiled and 18 observations were excluded from the analysis because they were below the limit of quantification (Table S3). Net drug killing over time, which reflected the effect of moxifloxacin in relation to the growth control, was calculated using Equation 1.

$$\text{Net drug killing}_{(t,j)} = \log_{10} \text{CFU}_{\text{MXF}(t,j)} - \overline{\log_{10} \text{CFU}_{\text{control}(t)}} \quad (1)$$

The net drug killing was analysed using nonlinear mixed effect modelling in NONMEM (v.7.4.3, Icon Development Solutions, Ellicott City, MD, USA).³⁴ Level 2 (L2) data item was implemented for technical replicates. A mono- and bi-exponential function (Equation 2 and Equation 3) were fitted to the net drug killing over time data.

$$\text{Net drug killing} = \log_{10} (e^{A_{\text{mono}}} \cdot e^{-\alpha_{\text{mono}} \cdot \text{Time}}) \quad (2)$$

$$\text{Net drug killing} = \log_{10} (e^{A_{\text{bi}}} \cdot e^{-\alpha_{\text{bi}} \cdot \text{Time}} + e^{B_{\text{bi}}} \cdot e^{-\beta_{\text{bi}} \cdot \text{Time}}) \quad (3)$$

where A_{mono} and A_{bi} represent the first intercept for mono- and bi-exponential models respectively, B_{bi} described the second intercept in a bi-exponential model, α_{mono} and α_{bi} are the first slope for mono- and bi-exponential models respectively and β_{bi} is the second slope of the bi-exponential models. The model evaluation was done based on likelihood ratio test with 5% significance level for nested model, goodness of fit plots and visual predictive check.

Once the base model was developed, the impact on bacterial killing of the different covariates were evaluated on the slope and intercept parameters (Equation 4) using stepwise covariate model implemented in PsN (version 5.3.1; Department of Pharmaceutical Biosciences, <http://psn.sourceforge.net>, Uppsala, Sweden). Bacterial adaptation times (1, 3 and 7 days), bacterial strains (H37Ra and H37Rv), cartridge size (medium and small) and sampling ports (S1, S2, S3 and S4) were evaluated as categorical covariates coded as fractional change to reference group (Equation 5). The PK parameters, that is, C_{max} , at Day 1 and Day 3, and area under curve 0–24 h (AUC_{0-24h}) of moxifloxacin at Day 1 and Day 3 from the different sampling ports, were evaluated as the continuous covariates following linear, power and exponential functions (Equations 6–8). The AUC_{0-24h} was calculated using *ncappc* package in R (v.4.1.3; R Foundation for Statistical Computing, Vienna, Austria).³⁵ Forward inclusion of covariates relations at $P < .05$ was performed followed by backward elimination at $P < .01$.

$$TVP_i = \theta_{\text{pop}} \cdot (\text{CovEffect}_{\text{Pcov}_i}) \quad (4)$$

$\text{CovEffect}_{\text{Pcov}_i}$ is the fractional change in the parameter due to the covariate in individual i . θ_{pop} is the population typical value of parameter P (TVP _{i}) for a subject i .

$$\text{CovEffect}_{\text{Pcov}_i} = \begin{cases} 1 & \text{if } cov_i \text{ at reference level} \\ 1 + \theta_{\text{Pcov}_1} & \text{if } cov_i \text{ at level 1} \\ 1 + \theta_{\text{Pcov}_2} & \text{if } cov_i \text{ at level 2} \\ \dots & \dots \end{cases} \quad (5)$$

θ_{Pcov_L} is the fixed effect that establishes the impact of belonging to level L relative to the reference level.

$$\text{CovEffect}_{\text{Pcov}_i} = 1 + \theta_{\text{Pcov}} \cdot (\text{cov}_i - \text{cov}_{\text{reference}}) \quad (6)$$

$$\text{CovEffect}_{\text{Pcov}_i} = \left(\frac{\text{cov}_i}{\text{cov}_{\text{reference}}} \right)^{\theta_{\text{Pcov}}} \quad (7)$$

$$\text{CovEffect}_{\text{Pcov}_i} = e^{\theta_{\text{Pcov}_1} \cdot (\text{cov}_i - \text{cov}_{\text{reference}})} \quad (8)$$

θ_{Pcov} is the covariate coefficient, cov_i is the value of the covariate of individual i , $\text{cov}_{\text{reference}}$ is the median covariate value.

In addition, the AUC_{0-t} ratio of the exposure between the ECS and ICS sampling port was calculated where 1.00 would indicate no difference in PK in the 2 ports (Equation 9).

$$AUC_{(0-t)} \text{ ECS/ICS} = \frac{AUC_{(0-t)} \text{ ECS}}{AUC_{(0-t)} \text{ ICS}} \quad (9)$$

In this study, we hypothesized that AUC_{0-t} in ECS and ICS were similar and thereby assumed they harboured the same bacterial killing when the AUC_{0-t} ECS/ICS was within the interval of 0.8–1.25. This approach and interval were adapted from the bioequivalence study criteria.^{36,37} A bioequivalence study is typically done to compare the PK of a new formulation of the same active substance as in the reference formulation. Bioequivalence limits are set to ensure the similarity in PK and give comparable in vivo performance in terms of safety and efficacy.^{36,37} In this work, we applied the bioequivalence criteria, that is, a difference in exposure higher than ± 0.2 in log normal distribution (corresponding to -0.20 to $+0.25$ in normal scale) where this is considered clinically relevant.

3 | RESULTS

3.1 | Cartridge size, fibres' composition and the presence of detergent in the assay media impact bacterial growth dynamics in the HFS-TB

Growth dynamics of *M. tuberculosis* H37Ra were initially assessed in a medium-size PS cartridge for 28 days in the HFS-TB and in a standard flask for comparison (Table S3). In the absence of tyloxapol, bacterial density rose by 2 orders of magnitude after 4 weeks of incubation; however, there were fewer cells in the cartridge than in the flask along the curve (Figure 1A). The culture in the cartridge gave rise to abundant bacterial clumps attached to the fibres that led to a poor collection of bacterial load in the samples taken from S2 and S3 ports, hence leading to an underestimation of the bacteria present in the cartridge and discrepancies between the \log_{10} CFU/mL measured from each port (Figure S1B). Conversely, as expected, the use of tyloxapol prevented the formation of clumps, thus allowing a homogeneous culture along the cartridge during the whole length of the assay (Figure S1C). Under these conditions, cells reached a higher bacterial density compared to the growth without detergent—9.89 \log_{10} CFU/mL vs. 6.83 \log_{10} CFU/mL, respectively—after 28 days of incubation. Cell density was also substantially higher than that obtained under static flask growth conditions (Figure 1A). It is worth mentioning that a schedule of cartridge homogenization to render an even bacterial population along the cartridge (S2–S3) was implemented from then on, thus making sampling from a single port (S3) representative to monitor bacterial growth.

Growth dynamics of *M. tuberculosis* H37Ra strain were then compared in different types of hollow-fibre cartridge materials. First, a medium-size cartridge sheltering PVDF fibres was used; this cartridge harbours a larger ECS volume and bigger fibre pores than the PS

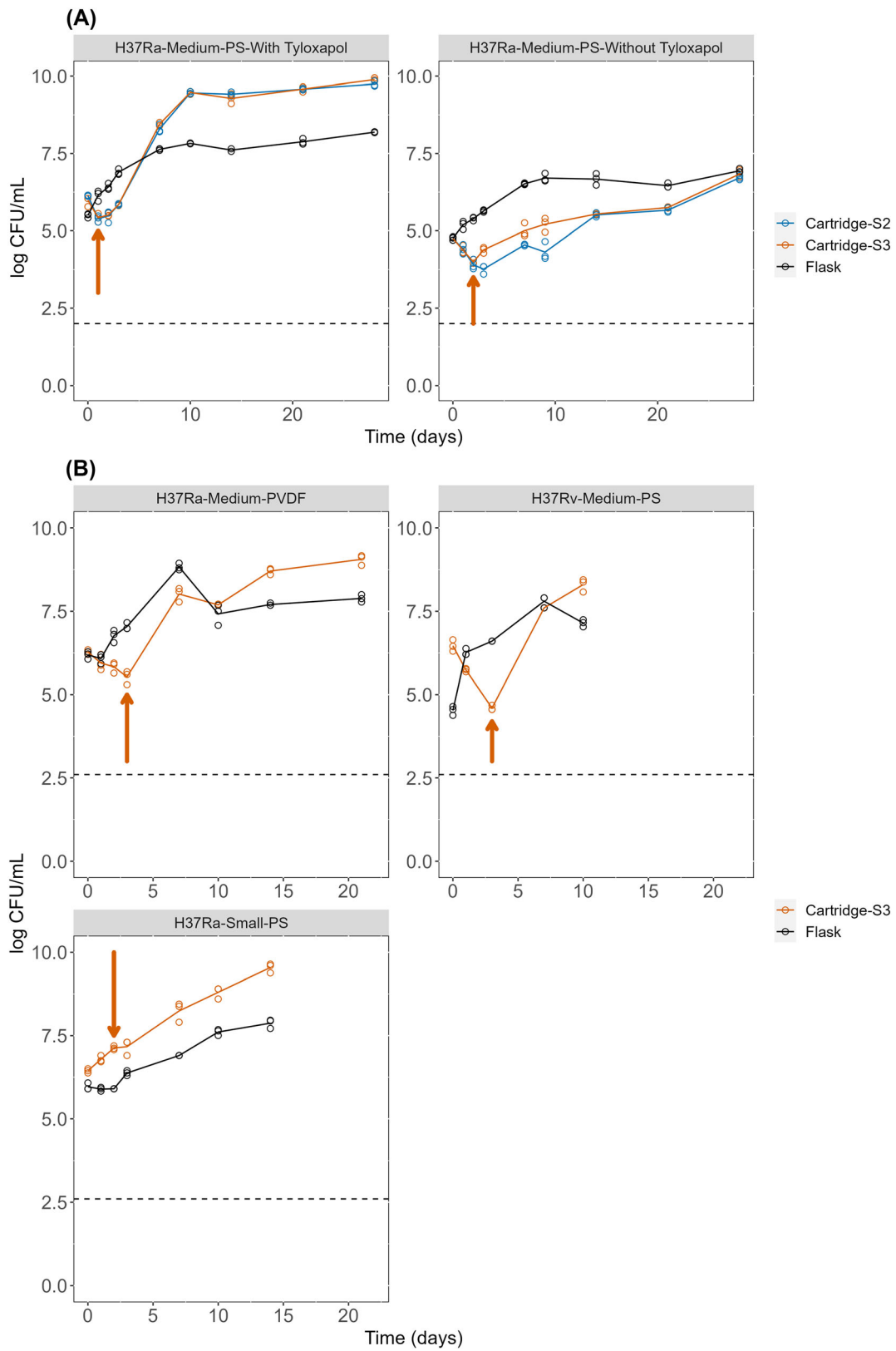


FIGURE 1 Legend on next page.

cartridge, which facilitates sampling. Net bacterial growth in the medium-size PVDF cartridge displayed almost 3 orders of magnitude after 21 days of incubation, and by the end of the experiment, the bacterial load in the cartridge had $\sim 1 \log_{10}$ CFU/mL more than the respective static culture in flask and approximately half a \log_{10} CFU/mL less than the medium-size PS cartridge (Figure 1B). Second, bacterial growth dynamics were studied in a small-size PS cartridge, whose ECS volume, surface area and oxygenation tubing are smaller than those of a medium-size cartridge, thereby having less system dead volume and faster medium renovation. After 14 days of incubation, growth in the small-size PS cartridge displayed $9.54 \log_{10}$ CFU/mL—a $1.67 \log_{10}$ difference over the static culture—which resembles the value reported in the medium-size PS cartridge at the same time-point ($9.28 \log_{10}$ CFU/mL; Figure 1B). Finally, growth of the pathogenic *M. tuberculosis* H37Rv strain was also characterized in a medium-size PS cartridge. To that end, the strain was cultivated both in a flask and in the HFS-TB cartridge for 10 days. Results were comparable to those obtained for the nonpathogenic *M. tuberculosis* H37Ra strain in the same type of cartridge. H37Rv bacterial growth in the cartridge spanned from $6.46 \log_{10}$ CFU/mL to 8.30 (Day 0 to Day 10), while H37Ra grew from $5.99 \log_{10}$ CFU/mL to 9.47 in the same time lapse (Figure 1B). It is worth noting that every cartridge's growth profile showed a similar tendency of slight decline in bacterial load during the first 3 days (Figure 1, orange arrow), followed by a logarithmic phase that surpassed cell densities obtained in static conditions. In the small-size PS cartridge a short lag phase could also be observed between Days 2 and 3 (Figure 1B). Altogether, these data highlight the need of robust characterization of bacterial growth dynamics in the chosen type of cartridge; this allows identification of the growth phase, and thus metabolic state, of the bacteria inside the system, before drug addition in the HFS-TB.

3.2 | Drug-fibres compatibility tests in the HFS-TB are needed before PKPD assays

Despite its paramount importance, verification of the compatibility of the drug of interest with the system and achievement of a particular PK profile are hardly reported in publications on HFS-TB.⁵ Herein, we checked the compatibility of 2 anti-TB drugs (moxifloxacin and rifampicin) with the materials of a hollow-fibre cartridge and the rest of the system.

We mimicked the total concentration in human plasma of a single moxifloxacin oral dose of 400 mg in a medium-size PS cartridge, in the absence of bacteria (Table S4). Moxifloxacin was compatible with

the PS cartridge and the whole system, because the expected C_{max} was reached both in the central compartment and in the ECS, and the antibiotic was cleared from the system as expected (Figure 2A). However, moxifloxacin concentrations in the ECS were slightly lower than those measured in the ICS, notably during the first samplings, which hints that a certain time lapse is needed to reach the equilibrium between both compartments (Figure 2A). Second, the total plasma concentration resulting from a single rifampicin oral dose of 600 mg was mimicked in a medium-size PS cartridge, in the absence of bacteria. Rifampicin was not compatible with the PS cartridges because concentration values from every compartment were far below the expected profile (Figure 2B), indicating unspecific binding of the drug to any of the components of the system.

3.3 | Impact of different HFS-TB parameters on moxifloxacin PKPD profile

The period of bacterial adaptation to the system prior to drug administration is not normally taken into consideration in HFS-TB experiments. In fact, our growth dynamics studies showed an at least 3 days delay in reaching bacterial log phase since cartridge inoculation (Figure 1). Thus, the impact of different bacterial adaptation periods (1, 3 and 7 days) prior to the first drug administration was evaluated on the bacterial killing effect (PD) of moxifloxacin against *M. tuberculosis* H37Ra. Bacterial killing seemed to be dependent on the length of the adaptation period, being more effective upon shorter adaptation times (Figure 3). By contrast, resistant mutants were not detected in any of the conditions when plated on $1.5 \mu\text{g/mL}$ moxifloxacin agar-containing plates.

The model-based analysis showed that moxifloxacin killing was best described using a bi-exponential function represented by a bi-phasic killing curve (Figure S2, Figure S3). The final parameter estimates can be found in Table S6. We found that the adaptation time had a significant impact on the baseline of slow killing and the rate of fast killing of moxifloxacin killing curve (Table S6, Figure S2, Figure S3). Faster and shorter initial killing occurred for 7 days adaptation time compared to 1 and 3 days adaptation time. Although the rate of fast killing for 3 days adaptation time was found to be 28.6% slower than 1 day adaptation time, the rate of slow killing was the same. Furthermore, the C_{max} and AUC did not influence the killing of bacteria based on the covariate analysis ($P > .05$).

Moxifloxacin concentrations reported in the ICS agreed with expected values, regardless of the presence and amount of bacteria in the ECS. In contrast, the higher bacterial density, the more

FIGURE 1 Growth dynamics of *Mycobacterium tuberculosis* in flasks and in the hollow-fibre system for tuberculosis. (A) *M. tuberculosis* H37Ra growth over time sampled from a flask and from the S2 and S3 ports of medium-size polysulfone (PS) cartridges in 7H9/OADC/Gly media with (left) and without (right) tyloxapol. (B) Bacterial growth (*M. tuberculosis* H37Ra and H37Rv) in different type of cartridges (medium-polyvinylidene fluoride [PVDF], medium-PS, small-PS) in 7H9/OADC/Gly/Tx media. \log_{10} colony forming units (CFU)/mL values of each experiment are provided in Table S3. Orange arrows point at the decline in the bacterial load that was observed inside the cartridges during the first 3 days of incubation. Open circles indicate experimental observations—3 technical replicates per time-point, the solid line represents the mean of observations and the dashed line represents the limit of quantification.

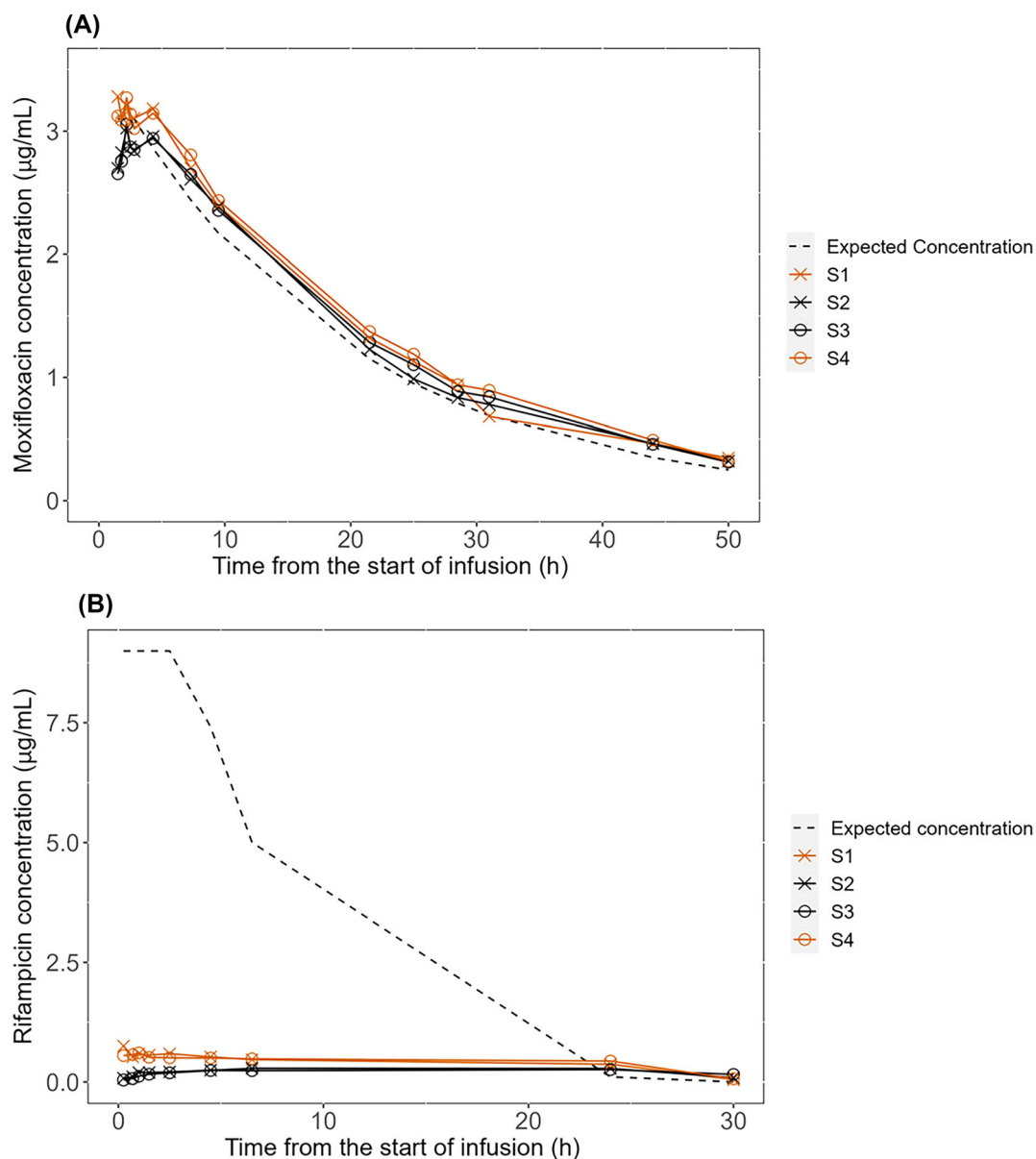


FIGURE 2 Drug-fibres compatibility tests of moxifloxacin and rifampicin in medium-size polysulfone cartridges. Observed pharmacokinetic profiles sampled from different sampling port at the extracapillary space (ECS) and intracapillary space (ICS) in the absence of bacteria, mimicking (A) human total plasma concentration after a single oral dose of 400 mg of moxifloxacin (B) human total plasma concentration after a single oral dose of 600 mg of rifampicin. The dashed line represents the expected concentration. The dilution started after 3 h. Moxifloxacin and rifampicin concentration values are provided in Table S4. S1 and S4 ports correspond to the ICS. S2 and S3 ports correspond to the ECS.

moxifloxacin accumulation was observed in the ECS (Figure 4). Most of the AUC ECS/ICS of measured moxifloxacin concentrations were within 0.8–1.25 except $\text{AUC}_{0-24\text{h}}(\text{day } 1)$ ECS/ICS in the 1 day adaptation time experiment (0.74) and $\text{AUC}_{0-24\text{h}}(\text{day } 3)$ ECS/ICS in the 7 days adaptation time experiment (1.34), as shown in Figure 4 and Table S7. This indicates that, in the 1 day adaptation time experiment, moxifloxacin had not reached the equilibrium in an early stage; while in the 7 day adaptation time experiment, accumulation was observed at a later time point, probably due to impaired drug diffusion at higher cell densities inside the cartridge. Alternatively, higher bacterial densities might entail higher amounts of bacterial components, that is, DNA

gyrases; since moxifloxacin binds these proteins³⁸, this may explain its accumulation in the ECS at later time points.

We next assessed the PKPD of moxifloxacin in the HFS-TB assay against 2 *M. tuberculosis* strains (H37Ra and H37Rv, 10^6 CFU/mL). They were exposed to 400 mg daily oral dosing of moxifloxacin in medium-size PS cartridges for 10 days, with 1 day of bacterial adaptation time. The model-based analysis showed that strain impacted the baseline of slow killing on the biphasic killing curve while the killing rates were the same for H37Ra and H37Rv (Figure S2, Figure S3 and Table S6). This resulted in an earlier onset of slow killing for H37Rv strain (Figure S3). For both strains, the bacterial load went below the

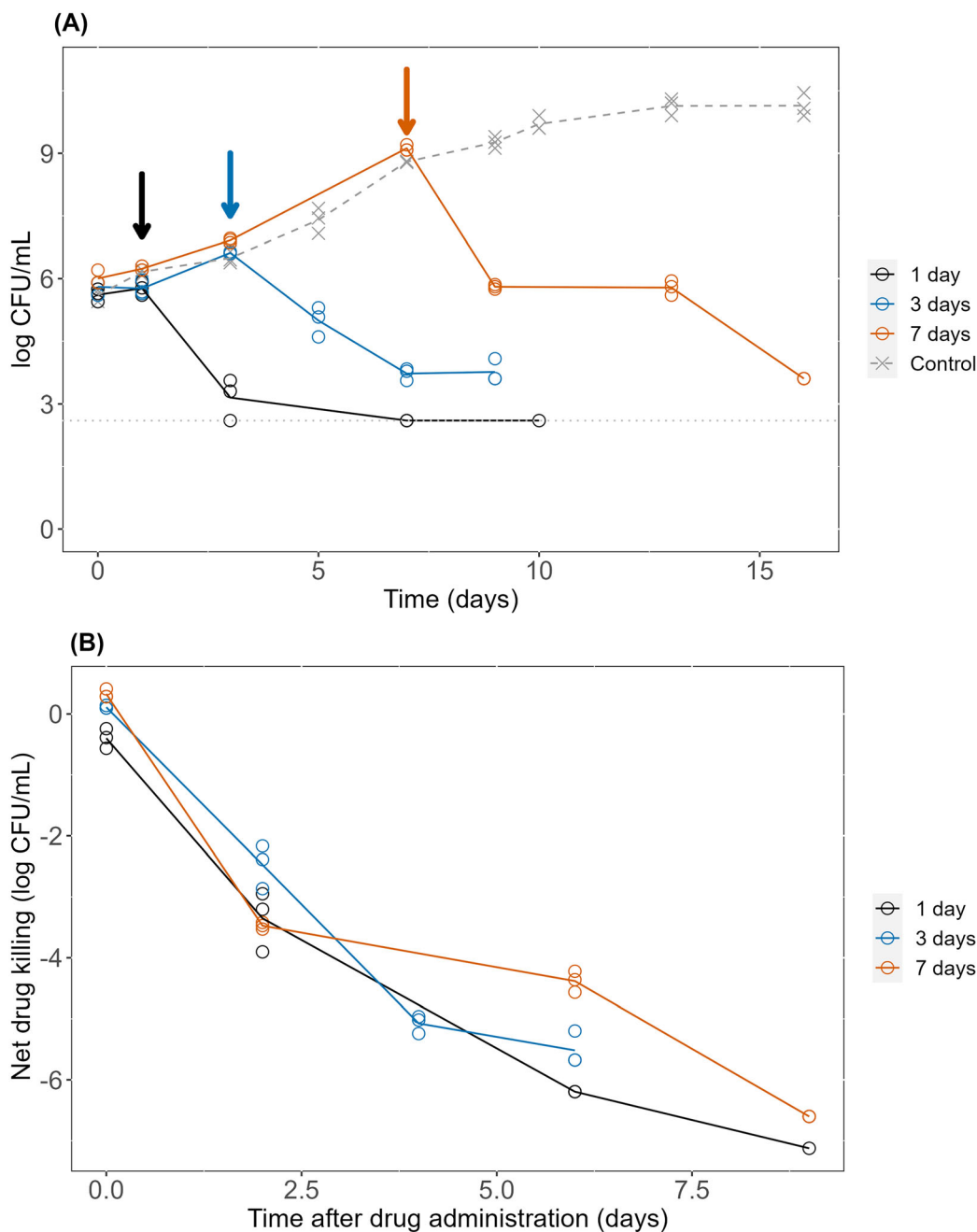
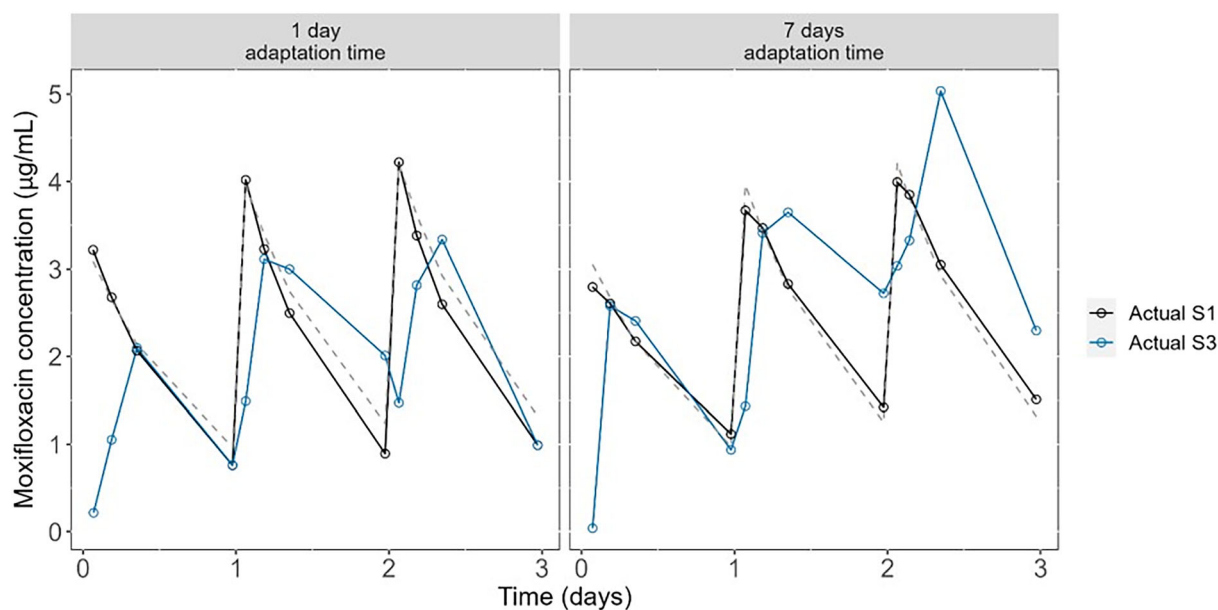


FIGURE 3 Moxifloxacin pharmacodynamics against *Mycobacterium tuberculosis* H37Ra in the hollow-fibre system for tuberculosis at different bacterial adaptation times. (A) Bacterial burden of *M. tuberculosis* H37Ra over time exposed to drug concentration mimicking human total plasma concentration after oral dose of moxifloxacin 400 mg daily for 10 days at different adaptation times. Colony forming units (CFU)/mL values are provided in Table S3. The solid and dashed lines represent the mean of the data, the grey dotted line indicates the limit of quantification, arrows indicate the first drug infusion, open circles and crosses indicate the observations—3 technical replicates per time-point. (B) Net drug killing vs. time after drug administration at different bacterial adaptation time. The solid line represents the mean of the data; open circles indicate the observed net drug killing—3 technical replicates per time-point.

limit of detection after 7 days of daily moxifloxacin dosing (Figure 5), and no resistance was detected. In both cases, the PK profile showed lower moxifloxacin concentration in the ECS compared to the expected concentration and the values obtained in the ICS (Figure 6). The AUC_{0-24h} (day 1) ECS/ICS (0.70) and AUC_{0-48h} ECS/ICS (0.77) for H37Rv strain experiment were outside 0.8–1.25 acceptable range

(Figure 6 and Table S8), indicating that at early time points the moxifloxacin concentration in the ECS did not reach the equilibrium.

Further, the same moxifloxacin PKPD HFS-TB assay was performed with *M. tuberculosis* H37Ra in a small-size PS cartridge. No major differences in bacterial killing upon moxifloxacin administration were observed between cartridge sizes (Figure 7). The model-based



AUC	AUC _{ECS} /AUC _{ICS} ratio	
	1 day adaptation time	7 days adaptation time
AUC _{0-24h} (day 1)	0.74*	0.90
AUC _{0-48h}	0.98	1.09
AUC _{0-72h}	0.97	1.19
AUC _{0-24h} (day 3)	0.95	1.34*

FIGURE 4 Moxifloxacin hollow-fibre system for tuberculosis pharmacokinetics (PK) in the presence of *Mycobacterium tuberculosis* H37Ra after different bacterial adaptation times. Moxifloxacin concentrations in S1 and S3 ports in medium-size polysulfone cartridges after 1 or 7 days of bacterial adaptation period. The expected concentration was shown as grey dashed line. Moxifloxacin concentrations are provided in Table S5. Simulated PK parameters are described in materials and methods. S1 and S3 ports correspond to the intracapillary space (ICS) and the extracapillary space (ECS) of the hollow-fibre system for tuberculosis, respectively. The table encompasses the area under the concentration–time curve (AUC) ratio between ECS and ICS; *: AUC ratios that are outside 0.80–1.25 range, indicating that the PK of moxifloxacin were different between the S1 and S3 ports.

analysis did not identify different cartridge sizes as a significant covariate on moxifloxacin bacterial killing (Table S6). PK profiles were accurately replicated for the small cartridge size. The AUC ECS/ICS in small cartridge (range 0.83–0.96) were still within 0.8–1.25 acceptance range (Table S9), but concentrations from ICS prone to exceed the expected, a tendency that increased over time (Figure 8). Most moxifloxacin concentrations from the ICS of the small-size cartridge were higher than those in the ECS (Figure 8, Table S5), which correlated with our previous standardization tests.

4 | DISCUSSION

The role of HFS-TB as a foremost preclinical tool to study PKPD profiles of antibiotic regimens against TB has been slowly but constantly growing.^{4,39,40} However, current literature lacks experimental detail

and standard procedures, a feature that, along with the high cost and infrastructure requisites of running HFS-TB, erects an access barrier to this technology for many research groups, thereby restricting the possibility to reproduce published data. A key review pointed out the need for best-practice principles to report HFS works,⁵ deepening the influence of unstandardized variables on PKPD outputs, such as the type of cartridge or the drug–fibres compatibility; variables that, to the best of our knowledge, have never been evaluated in former HFS-TB reports.

In this study, we assess the impact of several of these variables in the HFS-TB, using moxifloxacin as a case study. First, we uncovered the impact of detergent addition on the growth dynamics of *M. tuberculosis* H37Ra within the system. In this sense, we emphasize the need for a detergent supplement in the medium to disaggregate the clumps that bacteria formed inside the cartridge (Figure S1B,C), as well as frequently mixing the ECS content through S2 and S3 ports.

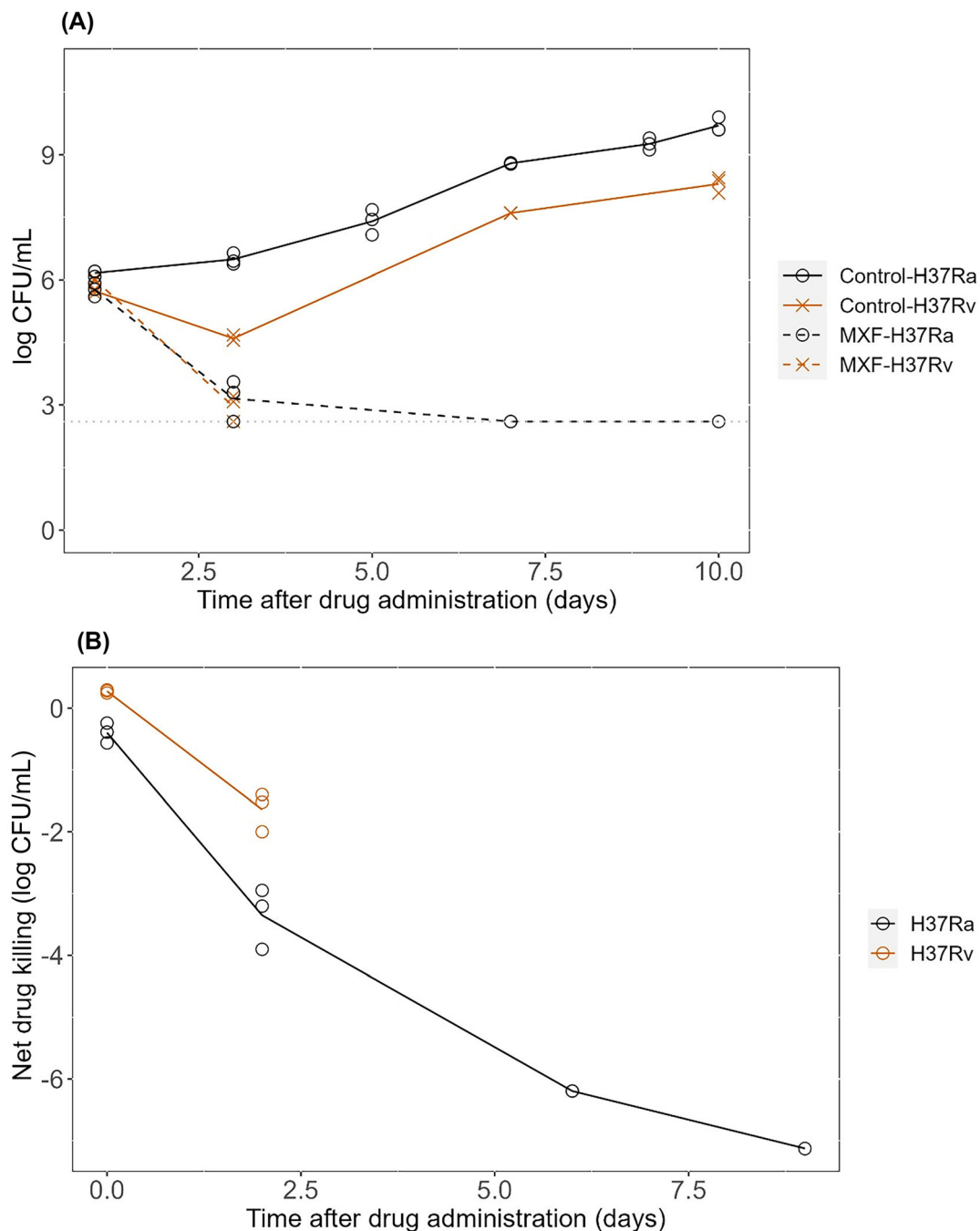
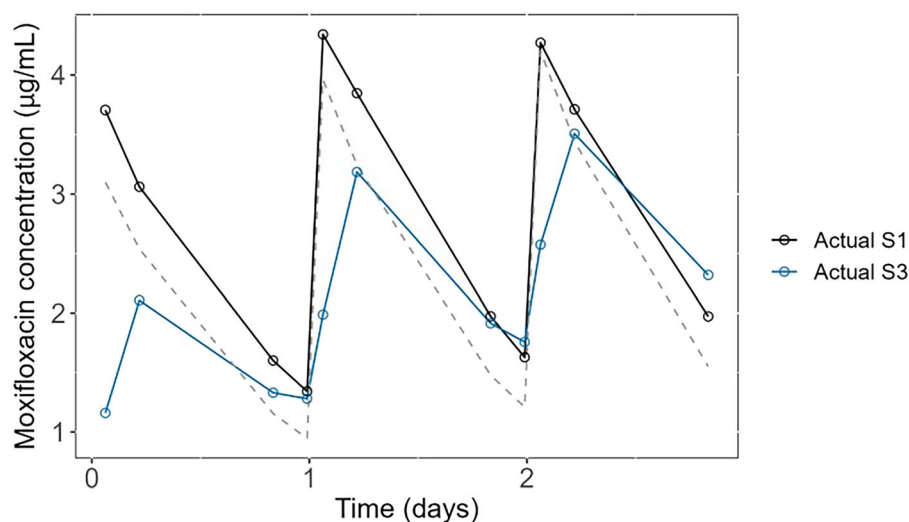


FIGURE 5 Moxifloxacin pharmacodynamics against different *Mycobacterium tuberculosis* strains in hollow-fibre system for tuberculosis medium-size polysulfone cartridges. (A) Bacterial burden of *M. tuberculosis* H37Ra strain or H37Rv strain over time with and without moxifloxacin exposure (mimicking total plasma concentration after 400 mg daily oral dosing of moxifloxacin in human for 10 days) after 1 day of bacterial adaptation period before the first drug administration. Colony forming units (CFU)/mL values are provided in Table S3. The solid and dashed lines represent the mean of the data, the grey dotted line indicates the limit of quantification and open circles indicate the observations—3 technical replicates per time-point. (B) Net drug killing vs. time after drug administration against *M. tuberculosis* H37Ra and H37Rv strain. The solid line represents the mean of the data; open circles indicate the observed net drug killing—3 technical replicates per time-point. MXF, moxifloxacin.

Without doing so, bacterial loads in the flask were higher than in the HFS-TB cartridges (Figure 1A), an unforeseen result because static conditions promote the accumulation of toxic metabolites that tend to diminish bacterial growth when fresh nutrients are consumed. Instead, the HFS-TB continuously provides those nutrients, so a

culture is likely to reach higher bacterial density in a cartridge than in static conditions. Since cartridges cannot be shaken or sonicated, manually mixing the ECS content on a regular basis (every other day) becomes essential, also for homogeneous distribution of the bacteria within the cartridge. Whether the presence of clumps and,



AUC	AUC _{ECS} /AUC _{ICS} ratio
AUC _{0-24h} (day 1)	0.70*
AUC _{0-48h}	0.77*
AUC _{0-72h}	0.84
AUC _{0-24h} (day 3)	0.97

FIGURE 6 Moxifloxacin hollow-fibre system for tuberculosis pharmacokinetics (PK) in the presence of *Mycobacterium tuberculosis* H37Rv in medium-size polysulfone cartridges. Moxifloxacin concentrations were obtained from S1 and S3 ports. The expected concentration was shown as grey dashed line. Moxifloxacin concentrations are provided in Table S5. Simulated PK parameters are described in materials and methods. S1 and S3 ports correspond to the intracapillary space (ICS) and the extracapillary space (ECS) of the hollow-fibre system for tuberculosis, respectively. The table encompasses the area under the concentration–time curve (AUC) ratio between ECS and ICS; *: AUC ratios that are outside 0.80–1.25 range indicate that the PK of moxifloxacin were different between the S1 and S3 ports.

consequently, different bacterial loads within cartridges could or not affect predictions of HFS-TB studies with a certain antibiotic has never been previously reported.

Bacterial growth dynamics were also characterized upon changing the fibres' material, the size of the cartridge and the bacterial strain. We found higher cell densities inside PS than PVDF cartridges (Figure 1B). Besides the fibres' nature, the main difference between PS and PVDF cartridges is the surface area, which is linked to the number of fibres and, therefore, the number of pores. PS cartridges have a surface area of 4000 cm², whereas PVDF cartridges harbour 880 cm². so this disparity may have allowed the proliferation of a higher bacterial content in PS than in PVDF cartridges. When comparing cartridges of different size, the opposite applied: cell density in the small-size PS cartridges on Day 14 was slightly higher than that in the medium-size PS cartridges (Figure 1B), the latter having a larger surface area (4000 vs. 450 cm²). This discrepancy might be due to the much shorter oxygenator tubing that the small-size cartridge possesses with respect to the medium-size cartridge: 0.65 vs. 4 m. This feature reduces system dead volume and it may entail faster medium renovation in the ECS, thereby providing fresh nutrients in a swifter cadence. However, these cartridges also differ in volume (3.2 mL in small-size vs. 20 mL in medium-size) and in the Duet pump rates (10 U small-size vs. 25 U medium-size); meaning that several variables might be responsible for such differences in bacterial growth. Ergo, our results highlight the importance of reporting all the details on the hollow-fibre cartridges.

We also observed that, within the conditions used in this work, the *M. tuberculosis* H37Rv strain reached lower cell density than *M. tuberculosis* H37Ra in the same cartridges, that is, medium-size PS

(Figure 1B, Table S3). This could be explained by the genetic dissimilitude between both strains⁴¹ and suggests that HFS-TB outcomes may also hinge on the strain. As a final note, our growth dynamics studies shared 2 common features: cell density (CFU/mL) inside the cartridges always outnumbered those in the control flasks, which is likely to be caused by the larger volume and continuous media refreshing in the cartridges, and/or the limited shaking in the flasks during the incubation⁴²; and a small decline on cartridge's bacterial load was consistently observed along the first 3 days in all the HFS-TB experiments (Figure 1). The reason behind this temporary drop could be that *M. tuberculosis* needs a certain time to adapt to the new environment inside the cartridge; a fact that should be contemplated when deciding the best moment to dispense a drug into the system. At this point, these results suggest that the assessment of qualitative and quantitative bacterial dynamics without drug treatment in the HFS-TB may be of interest because their diverse traits can modify bacterial density; a potential bias that modelling predictions should not overlook when analysing and comparing data between HFS-TB works performed with different set-ups.

Next, we tested the suitability of PS fibres, in absence of bacteria, to emulate moxifloxacin and rifampicin PK profiles. It is worth remarking that, in a former study, rifampicin was successfully used in a HFS experiment with cellulose cartridges.⁴³ However, its use with PS cartridges has never been reported elsewhere. Using a single dose of both drugs, our data indicated that moxifloxacin was compatible with PS fibres, whereas rifampicin was not (Figure 2). Hence, our data emphasize the importance of assessing drug-cartridge's fibre compatibility before addressing PKPD studies. Moreover, we urge researchers to routinely report these materials' suitability tests and other HFS

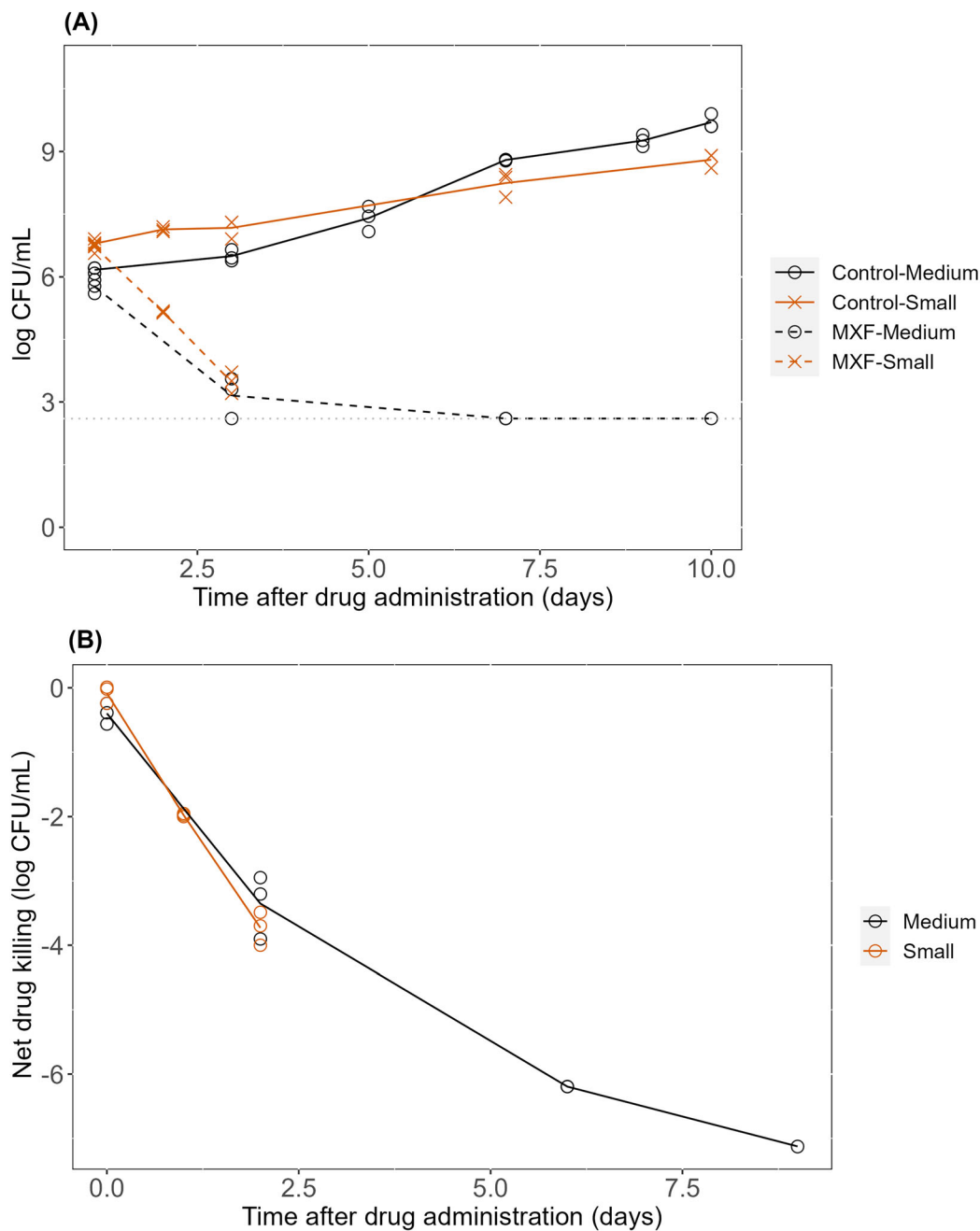
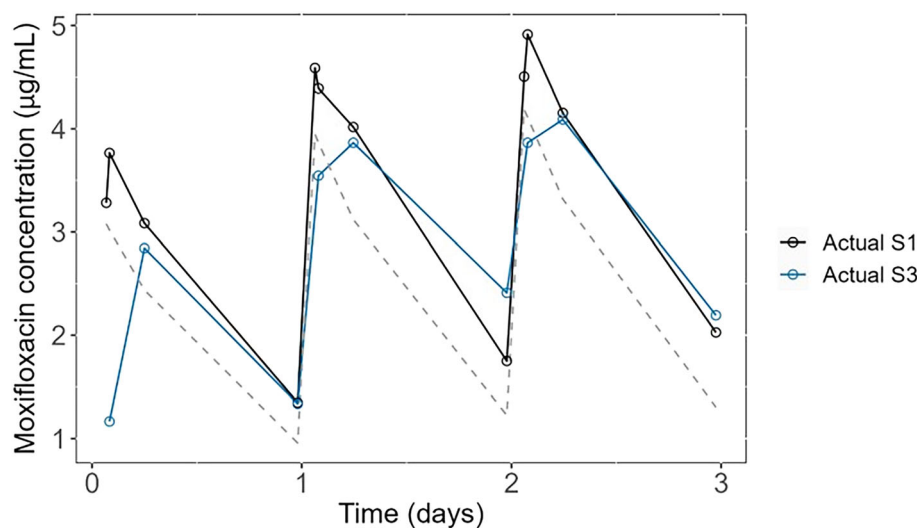


FIGURE 7 Moxifloxacin pharmacodynamics against *Mycobacterium tuberculosis* H37Ra in different polysulfone cartridge's sizes. (A) Bacterial burden of *M. tuberculosis* H37Ra strain over time in small- and medium-size polysulfone cartridges with and without moxifloxacin exposure (mimicking total plasma concentration after 400 mg daily oral dosing of moxifloxacin for 10 days) after 1 day of bacterial adaptation period before the first drug administration. Colony forming units (CFU)/mL values are provided in Table S3. The solid and dashed lines represent the mean of the data, the grey dotted line indicates the limit of quantification, open circles and crosses indicate the observations—3 technical replicates per time-point. (B) Net drug killing vs. time after drug administration in small- and medium-size polysulfone cartridges with H37Ra strain. The solid line represents the mean of the data and open circles indicate the observed net drug killing—3 technical replicates per time-point. MXF, moxifloxacin.

settings and modifications performed to achieve the desired PK profiles. Additionally, the PK assays in our study showed that the measured moxifloxacin concentrations from the ECS did not match the predicted profile as rigorously as those from the ICS, especially during the first steps of the experiments, which might suggest the need for

an equilibrium lapse after drug infusion (Figure 2). At this stage we must emphasize that, customarily, HFS-TB studies normally only report drug levels at the central compartment (ICS), thereby neglecting the ECS, where bacteria are effectively exposed to the antibiotic.^{10,27,40,44} In light of our data, one should not assume a perfect



AUC	AUC _{ECS} /AUC _{ICS} ratio
AUC _{0-24h} (day 1)	0.83
AUC _{0-48h}	0.95
AUC _{0-72h}	0.96
AUC _{0-24h} (day 3)	0.98

FIGURE 8 Moxifloxacin hollow-fibre system for tuberculosis pharmacokinetics (PK) in the presence of *Mycobacterium tuberculosis* H37Ra in small-size polysulfone cartridge. Moxifloxacin concentrations were obtained from S1 and S3 ports. The expected concentration was shown as grey dashed line. Moxifloxacin concentrations are provided in Table S5. Simulated PK parameters are described in materials and methods. S1 and S3 ports correspond to the intracapillary space (ICS) and the extracapillary space (ECS) of the hollow-fibre system for tuberculosis, respectively. The table encompasses the area under the concentration–time curve (AUC) ratio between ECS and ICS.

correspondence between the drug concentration in the central compartment and the lumen of the cartridges.

We then examined the potential effect that bacterial adaptation time prior to drug dosing (i.e. the amount of bacteria and their growth phase) may exert on PKPD assays for 10 days with moxifloxacin against the *M. tuberculosis* H37Ra strain. Our study found that the length of the bacterial adaptation time significantly impacted the moxifloxacin bacterial killing (Figure 3, Table S6), meaning that moxifloxacin probably killed differently across bacterial subpopulations. A study from Clewe *et al.*,⁴⁵ revealed that the proportion of different mycobacterial subpopulation changes over time. Therefore, a distinct bacterial adaptation time is likely to entail different proportions of subpopulations. In addition, a static time-kill study from Sulochana *et al.*,⁴⁶ showed faster moxifloxacin killing in exponential phase culture than in stationary phase (4 weeks) culture, which again indicates that moxifloxacin worked differently on different bacterial subpopulation. Moreover, the different cell density depending on the adaption time, could also be behind the impact on moxifloxacin action.²⁹ In fact, it has been observed that the killing exerted by this quinolone on other bacteria is contingent on the bacterial burden.⁴⁷ Altogether, this information suggests that bacterial adaptation times prior to drug dosing are a key factor to consider before setting up a HFS-TB experiment. Selection of a bacterial adaptation time would depend on the experimental question to be answer, which will dictate the simulation of the appropriate growth phase and population's status of *M. tuberculosis*.

Subsequently, we determined that PK sampling from ECS or ICS in the HFS-TB may also impact PKPD outcomes (Figure 4). As discussed above, the longer the adaptation time, the higher the bacterial density inside the cartridge, which may compromise drug permeability

and distribution through the fibres, thereby explaining the correlation between PK and bacterial adaptation time. In light of these notions, one should be careful when dealing with drugs whose physicochemical properties could entail unspecific binding to the cartridge and, consequently, alter drug concentration in the ECS. Therefore, we advise that preliminary tests should be made to unveil the actual drug concentrations that bacteria face inside the ECS in the cartridges and to measure the equilibrium time the compound needs to reach the desired C_{max} in the ECS.

In addition, we evaluated the impact of the bacterial strain (H37Ra vs. H37Rv) on the moxifloxacin PKPD in the HFS-TB (Figure 5). The PD profile from the *M. tuberculosis* H37Rv strain with 1 day of bacterial adaption period concurred with previous data.^{12,27} Although we identified that strain impacted the onset of the slow killing in the biphasic killing curve, killing rates were the same (Figure S2, Figure S3, Table S6), suggesting that traceability was not affected between experiments with nonvirulent and virulent strains, which sides with former data.⁴⁸ Nonetheless, our results suggest that evaluating different isolates beyond the laboratory H37Rv strain in the HFS-TB is advisable; a broader assortment of strains would release more accurate predictions for regimen recommendations. Particularly, strains from different lineages, or MDR and/or XDR strains with dissimilar resistance patterns, might be included in order to improve the robustness of the data and to cover a larger number of potential TB infections. Finally, we appraised the role of cartridge's size on the moxifloxacin PKPD with *M. tuberculosis* H37Ra, finding it to be statistically nonsignificant (Figure 7, Table S5).

One of the limitations of HFS-TB is the sheer cost of cartridges, which limits the availability of performing multiple biological

replicates. In our work, this may affect the robustness of the PD results. Nevertheless, we overcome this limitation by applying in silico modelling tools pooling different experiments in order to boost the robustness of our conclusions.

5 | CONCLUSIONS

This work constitutes the first semisystematic study on the impact of the most relevant variables in the HFS-TB field. In this sense, we have shown that bacterial adaptation times influenced moxifloxacin bacterial killing in HFS-TB. When variations were detected in this parameter, the AUC ratio in the different sampling compartments differed, which can impact the quantified PKPD relationships in these experiments. The results also highlight the need of providing essential information for key procedures and parameters, which have been often disregarded when reporting PKPD experiments in the HFS-TB. By doing so, the HFS-TB field will make a sizable step towards reaching gold standards that this preclinical tool should require for publication and ulterior clinical extrapolation to design Phase II/III trials for anti-TB drugs.

AUTHOR CONTRIBUTIONS

CRediT (Contributor Roles Taxonomy) has been applied for author contribution.

Conceptualization: Santiago Ramón-García, Ainhoa Lucía. **Data curation:** Diana A. Aguilar-Ayala, Fernando Sanz-García, Marie Sylvianne Rabodoarivelo and Rebeca Bailo. **Formal analysis:** Diana A. Aguilar-Ayala, Fernando Sanz-García, Marie Sylvianne Rabodoarivelo and Budi O. Susanto. **Funding acquisition:** Ulrika S. H. Simonsson and Santiago Ramón-García. **Investigation:** Diana A. Aguilar-Ayala, Fernando Sanz-García, Marie Sylvianne Rabodoarivelo, Rebeca Bailo and Maxime R. Eveque-Mourroux. **Methodology:** Diana A. Aguilar-Ayala, Fernando Sanz-García, Marie Sylvianne Rabodoarivelo and Ainhoa Lucía. **Project administration:** Ulrika S. H. Simonsson, Santiago Ramón-García and Ainhoa Lucía. **Resources:** Diana A. Aguilar-Ayala and Ainhoa Lucía. **Supervision:** Nicolas Willand, Ulrika S. H. Simonsson, Santiago Ramón-García and Ainhoa Lucía. **Visualization:** Diana A. Aguilar-Ayala, Fernando Sanz-García, Marie Sylvianne Rabodoarivelo and Budi O. Susanto. **Writing—original draft:** Fernando Sanz-García, Santiago Ramón-García and Budi O. Susanto. **Writing—review and editing:** Diana A. Aguilar-Ayala, Fernando Sanz-García, Marie Sylvianne Rabodoarivelo, Budi O. Susanto, Maxime R. Eveque-Mourroux, Ulrika S. H. Simonsson, Santiago Ramón-García and Ainhoa Lucía. All authors read and approved the final version of the document.

ACKNOWLEDGEMENTS

We would like to thank the technical support of Ana Picó Marco from the University of Zaragoza.

This work has received support from the Government of Aragon, Spain (Ref. LMP132_18; Gobierno de Aragón y Fondos Feder de la Unión Europea ‘Construyendo Europa desde Aragón’) to S.R.G. and from the Innovative Medicines Initiatives 2 Joint Undertaking (grant

No 853989) to N.W., U.S.H.S. and S.R.G. The JU receives support from the European Union's Horizon 2020 Research and Innovation Programme and EFPIA and Global Alliance for TB Drug Development Non-Profit Organization, Bill & Melinda Gates Foundation, University of Dundee. <http://www.imi.europa.eu>.

CONFLICT OF INTEREST STATEMENT

None.

DATA AVAILABILITY STATEMENT

The data that support the findings of this study are available from the corresponding author upon reasonable request.

ORCID

Fernando Sanz-García  <https://orcid.org/0000-0001-8238-2388>

Santiago Ramón-García  <https://orcid.org/0000-0002-8480-0325>

REFERENCES

- European Medicines Agency. Qualification Opinion In-vitro Hollow Fiber System Model of Tuberculosis (HSF-TB). Available online. 2015.
- Cavaleri M, Manolis E. Hollow fiber system model for tuberculosis: the European Medicines Agency experience. *Clin Infect Dis*. 2015;61(Suppl 1):S1-S4. doi:[10.1093/cid/civ484](https://doi.org/10.1093/cid/civ484)
- Romero K, Clay R, Hanna D. Strategic regulatory evaluation and endorsement of the hollow fiber tuberculosis system as a novel drug development tool. *Clin Infect Dis*. 2015;61(Suppl 1):S5-S9. doi:[10.1093/cid/civ424](https://doi.org/10.1093/cid/civ424)
- Maitra A, Solanki P, Sadouki Z, McHugh TD, Kloprogge F. Improving the drug development pipeline for mycobacteria: modelling antibiotic exposure in the hollow fibre infection model. *Antibiotics*. 2021;10(12):1515. doi:[10.3390/antibiotics10121515](https://doi.org/10.3390/antibiotics10121515)
- Sadouki Z, McHugh TD, Aarnoutse R, et al. Application of the hollow fibre infection model (HFIM) in antimicrobial development: a systematic review and recommendations of reporting. *J Antimicrob Chemother*. 2021;76(9):2252-2259. doi:[10.1093/jac/dkab160](https://doi.org/10.1093/jac/dkab160)
- Gloede J, Scheerans C, Derendorf H, Kloft C. In vitro pharmacodynamic models to determine the effect of antibacterial drugs. *J Antimicrob Chemother*. 2010;65(2):186-201. doi:[10.1093/jac/dkp434](https://doi.org/10.1093/jac/dkp434)
- Velkov T, Bergen PJ, Lora-Tamayo J, Landersdorfer CB, Li J. PK/PD models in antibacterial development. *Curr Opin Microbiol*. 2013;16(5):573-579. doi:[10.1016/j.mib.2013.06.010](https://doi.org/10.1016/j.mib.2013.06.010)
- Gumbo T, Pasipanodya JG, Romero K, Hanna D, Nuermberger E. Forecasting accuracy of the hollow fiber model of tuberculosis for clinical therapeutic outcomes. *Clin Infect Dis*. 2015;61(Suppl 1):S25-S31. doi:[10.1093/cid/civ427](https://doi.org/10.1093/cid/civ427)
- Svensson RJ, Gillespie SH, Simonsson USH. Improved power for TB phase IIa trials using a model-based pharmacokinetic-pharmacodynamic approach compared with commonly used analysis methods. *J Antimicrob Chemother*. 2017;72(8):2311-2319. doi:[10.1093/jac/dkx129](https://doi.org/10.1093/jac/dkx129)
- Gumbo T, Louie A, Deziel MR, Parsons LM, Salfinger M, Drusano GL. Selection of a moxifloxacin dose that suppresses drug resistance in mycobacterium tuberculosis, by use of an in vitro pharmacodynamic infection model and mathematical modeling. *J Infect Dis*. 2004;190(9):1642-1651. doi:[10.1086/424849](https://doi.org/10.1086/424849)
- van Rijn SP, Srivastava S, Wessels MA, van Soolingen D, Alffenaar JC, Gumbo T. Sterilizing effect of ertapenem-clavulanate in a hollow-fiber model of tuberculosis and implications on clinical dosing. *Antimicrob Agents Chemother*. 2017;61(9):e02039-16. doi:[10.1128/AAC.02039-16](https://doi.org/10.1128/AAC.02039-16)

12. Drusano GL, Rogers S, Brown D, et al. Dose fractionation of moxifloxacin for treatment of tuberculosis: impact of dosing interval and elimination half-life on microbial kill and resistance suppression. *Antimicrob Agents Chemother.* 2021;65(4):e02533-20. doi:10.1128/AAC.02533-20
13. Kempker RR, Barth AB, Vashakidze S, et al. Cavitory penetration of levofloxacin among patients with multidrug-resistant tuberculosis. *Antimicrob Agents Chemother.* 2015;59(6):3149-3155. doi:10.1128/AAC.00379-15
14. Heinrichs MT, Vashakidze S, Nikolaishvili K, et al. Moxifloxacin target site concentrations in patients with pulmonary TB utilizing microdialysis: a clinical pharmacokinetic study. *J Antimicrob Chemother.* 2018;73(2):477-483. doi:10.1093/jac/dkx421
15. Pasipanodya J, Gumbo T. An oracle: antituberculosis pharmacokinetics-pharmacodynamics, clinical correlation, and clinical trial simulations to predict the future. *Antimicrob Agents Chemother.* 2011;55(1):24-34. doi:10.1128/AAC.00749-10
16. Gumbo T, Lenaerts AJ, Hanna D, Romero K, Nuermberger E. Nonclinical models for antituberculosis drug development: a landscape analysis. *J Infect Dis.* 2015;211(Suppl 3):S83-S95. doi:10.1093/infdis/jiv183
17. Gumbo T, Angulo-Barturen I, Ferrer-Bazaga S. Pharmacokinetic-pharmacodynamic and dose-response relationships of antituberculosis drugs: recommendations and standards for industry and academia. *J Infect Dis.* 2015;211(Suppl 3):S96-S106. doi:10.1093/infdis/jiu610
18. Srivastava S, Deshpande D, Magombede G, et al. Duration of pretomanid/moxifloxacin/pyrazinamide therapy compared with standard therapy based on time-to-extinction mathematics. *J Antimicrob Chemother.* 2020;75(2):392-399. doi:10.1093/jac/dkz460
19. Deshpande D, Srivastava S, Nuermberger E, Pasipanodya JG, Swaminathan S, Gumbo T. A faropenem, linezolid, and moxifloxacin regimen for both drug-susceptible and multidrug-resistant tuberculosis in children: FLAME path on the milky way. *Clin Infect Dis.* 2016;63(suppl 3):S95-S101. doi:10.1093/cid/ciw474
20. Deshpande D, Srivastava S, Nuermberger E, et al. Multiparameter responses to tedizolid monotherapy and moxifloxacin combination therapy models of children with intracellular tuberculosis. *Clin Infect Dis.* 2018;67(suppl_3):S342-S348. doi:10.1093/cid/ciy612
21. Srivastava S, van Zyl J, Cirrincione K, et al. Evaluation of ceftriaxone plus avibactam in an intracellular hollow fiber model of tuberculosis: implications for the treatment of disseminated and meningeal tuberculosis in children. *Pediatr Infect Dis J.* 2020;39(12):1092-1100. doi:10.1097/INF.0000000000002857
22. Gosling RD, Uiso LO, Sam NE, et al. The bactericidal activity of moxifloxacin in patients with pulmonary tuberculosis. *Am J Respir Crit Care Med.* 2003;168(11):1342-1345. doi:10.1164/rccm.200305-682OC
23. Nuermberger EL, Yoshimatsu T, Tyagi S, et al. Moxifloxacin-containing regimen greatly reduces time to culture conversion in murine tuberculosis. *Am J Respir Crit Care Med.* 2004;169(3):421-426. doi:10.1164/rccm.200310-1380OC
24. Perveen S, Kumari D, Singh K, Sharma R. Tuberculosis drug discovery: progression and future interventions in the wake of emerging resistance. *Eur J Med Chem.* 2022;229:114066. doi:10.1016/j.ejmech.2021.114066
25. Maitra A, Bates S, Kolvekar T, Devarajan PV, Guzman JD, Bhakta S. Repurposing—a ray of hope in tackling extensively drug resistance in tuberculosis. *Int J Infect Dis.* 2015;32:50-55. doi:10.1016/j.ijid.2014.12.031
26. Ginsburg AS, Lee J, Woolwine SC, Grosset JH, Hamzeh FM, Bishai WR. Modeling in vivo pharmacokinetics and pharmacodynamics of moxifloxacin therapy for mycobacterium tuberculosis infection by using a novel cartridge system. *Antimicrob Agents Chemother.* 2005;49(2):853-856. doi:10.1128/AAC.49.2.853-856.2005
27. Drusano GL, Sgambati N, Eichas A, Brown DL, Kulawy R, Louie A. The combination of rifampin plus moxifloxacin is synergistic for suppression of resistance but antagonistic for cell kill of *Mycobacterium tuberculosis* as determined in a hollow-fiber infection model. *MBio.* 2010;1(3):e00139-10. doi:10.1128/mBio.00139-10
28. Mason AB, Dartois V. Drug sensitivity testing of mycobacterium tuberculosis growing in a hollow fiber bioreactor. *Methods Mol Biol.* 2021;2314:715-731. doi:10.1007/978-1-0716-1460-0_31
29. van Wijk RC, Lucia A, Sudhakar PK, et al. Implementing best practices on data generation and reporting of *Mycobacterium tuberculosis* in vitro assays within the ERA4TB consortium. *iScience.* 2023;26(4):106411. doi:10.1016/j.isci.2023.106411
30. Karazniewicz-Lada M, Kosicka-Noworzyn K, Rao P, et al. New approach to rifampicin stability and first-line anti-tubercular drug pharmacokinetics by UPLC-MS/MS. *J Pharm Biomed Anal.* 2023;235:115650. doi:10.1016/j.jpba.2023.115650
31. El-Yazbi AF, Aboukhalil FM, Khamis EF, Elkhatib MAW, El-Sayed MA, Youssef RM. Simple simultaneous determination of moxifloxacin and metronidazole in complex biological matrices. *RSC Adv.* 2022;12(25):15694-15704. doi:10.1039/d2ra01631a
32. Kim MK, Nightingale CH. Pharmacodynamics and pharmacokinetics of the fluoroquinolones. In: Andriole VT, ed. *The quinolones*. 3rd ed. 2000:169-202. doi:10.1016/B978-012059517-4/50006-4
33. Stott KE, Pertinez H, Sturkenboom MGG, et al. Pharmacokinetics of rifampicin in adult TB patients and healthy volunteers: a systematic review and meta-analysis. *J Antimicrob Chemother.* 2018;73(9):2305-2313. doi:10.1093/jac/dky152
34. Beal S. L. SLB, Boeckmann A. J., Bauer R. J. NONMEM 7.4.3 users guides (1989–2018). Icon Development Solutions 2018;
35. Acharya C, Hooker AC, Turkyilmaz GY, Jonsson S, Karlsson MO. A diagnostic tool for population models using non-compartmental analysis: the ncapc package for R. *Comput Methods Programs Biomed.* 2016;127:83-93. doi:10.1016/j.cmpb.2016.01.013
36. European Medicine Agency, Guideline on the Investigation of Bioequivalence. Accessed May 12, 2023. https://www.ema.europa.eu/en/documents/scientific-guideline/guideline-investigation-bioequivalence-rev1_en.pdf
37. Food and Drug Administration, Guideline for Industry: Statistical Approaches to Establishing Bioequivalence. Accessed May 12, 2023. <https://www.fda.gov/media/70958/download>
38. Chan PF, Srikannathasan V, Huang J, et al. Structural basis of DNA gyrase inhibition by antibacterial QPT-1, anticancer drug etoposide and moxifloxacin. *Nat Commun.* 2015;6(1):10048. doi:10.1038/ncomms10048
39. Srivastava S, Sherman C, Meek C, Leff R, Gumbo T. Pharmacokinetic mismatch does not lead to emergence of isoniazid- or rifampin-resistant mycobacterium tuberculosis but to better antimicrobial effect: a new paradigm for antituberculosis drug scheduling. *Antimicrob Agents Chemother.* 2011;55(11):5085-5089. doi:10.1128/AAC.00269-11
40. Deshpande D, Srivastava S, Nuermberger E, Pasipanodya JG, Swaminathan S, Gumbo T. Concentration-dependent synergy and antagonism of linezolid and moxifloxacin in the treatment of childhood tuberculosis: the dynamic duo. *Clin Infect Dis.* 2016;63(suppl 3):S88-S94. doi:10.1093/cid/ciw473
41. Brosch R, Philipp WJ, Stavropoulos E, Colston MJ, Cole ST, Gordon SV. Genomic analysis reveals variation between mycobacterium tuberculosis H37Rv and the attenuated M. Tuberculosis H37Ra strain. *Infect Immun.* 1999;67(11):5768-5774. doi:10.1128/IAI.67.11.5768-5774.1999
42. Nazarova EV, Russell DG. Growing and handling of mycobacterium tuberculosis for macrophage infection assays. *Methods Mol Biol.* 2017;1519:325-331. doi:10.1007/978-1-4939-6581-6_22
43. Ruth MM, Raaijmakers J, van den Hombergh E, et al. Standard therapy of *Mycobacterium avium* complex pulmonary disease shows limited efficacy in an open source hollow fibre system that simulates human plasma and epithelial lining fluid pharmacokinetics. *Clin Microbiol Infect.* 2022;28(3):448 e1-448 e7. doi:10.1016/j.cmi.2021.07.015

44. Gumbo T, Srivastava S, Deshpande D, et al. Hollow-fibre system model of tuberculosis reproducibility and performance specifications for best practice in drug and combination therapy development. *J Antimicrob Chemother.* 2023;78(4):953-964. doi:[10.1093/jac/dkad029](https://doi.org/10.1093/jac/dkad029)
45. Clewe O, Aulin L, Hu Y, Coates AR, Simonsson US. A multistate tuberculosis pharmacometric model: a framework for studying anti-tubercular drug effects in vitro. *J Antimicrob Chemother.* 2016;71(4):964-974. doi:[10.1093/jac/dkv416](https://doi.org/10.1093/jac/dkv416)
46. Sulochana S, Mitchison DA, Kubendiren G, Venkatesan P, Paramasivan CN. Bactericidal activity of moxifloxacin on exponential and stationary phase cultures of mycobacterium tuberculosis. *J Chemother.* 2009;21(2):127-134. doi:[10.1179/joc.2009.21.2.127](https://doi.org/10.1179/joc.2009.21.2.127)
47. Bowker KE, Garvey MI, Noel AR, Tomaselli SG, Macgowan AP. Comparative antibacterial effects of moxifloxacin and levofloxacin on *Streptococcus pneumoniae* strains with defined mechanisms of resistance: impact of bacterial inoculum. *J Antimicrob Chemother.* 2013;68(5):1130-1138. doi:[10.1093/jac/dks537](https://doi.org/10.1093/jac/dks537)
48. Heinrichs MT, May RJ, Heider F, et al. Mycobacterium tuberculosis strains H37ra and H37rv have equivalent minimum inhibitory concentrations to most antituberculosis drugs. *Int J Mycobacteriol.* 2018;7(2):156-161. doi:[10.4103/ijmy.ijmy_33_18](https://doi.org/10.4103/ijmy.ijmy_33_18)

SUPPORTING INFORMATION

Additional supporting information can be found online in the Supporting Information section at the end of this article.

How to cite this article: Aguilar-Ayala DA, Sanz-García F, Rabodoarivelo MS, et al. Evaluation of critical parameters in the hollow-fibre system for tuberculosis: A case study of moxifloxacin. *Br J Clin Pharmacol.* 2024;1-17. doi:[10.1111/bcp.16068](https://doi.org/10.1111/bcp.16068)